Investigating the composition of the gut microbiome in murine polytrauma and hemorrhagic shock

Sandra A. Appiah

Defense date: April 1, 2020

Molecular, Cellular, and Developmental Biology

University of Colorado Boulder

Thesis Advisor:

Dr. Christopher A. Lowry, Department of Integrative Physiology

Defense Committee:

Dr. Christopher A. Lowry, Department of Integrative Physiology

Dr. Brian DeDecker, Department of Molecular, Cellular, and Developmental Biology

Dr. Nancy Guild, Department of Molecular, Cellular, and Developmental Biology

Dr. Heidi Day, Department of Psychology and Neuroscience

Table of Contents

Abstract **2**

Introduction **3**

Materials and Methods **5**

Animals 5

Induction of PT and HS 6

Plasma, bronchoalveolar lavage (BAL), and fecal endpoints 7

Preparation of BAL fluids 8

Jejunum and colon mucus extraction and homogenization of jejunum and colon tissue 9

Protein assay 9

Enzyme-linked immunosorbent assay (ELISA) 9

Quantification of plasma creatinine 10

Bacterial DNA extraction and generation of 16S rRNA gene V4 amplicons 11

16S rRNA gene sequence and data preparation 12

Microbiome data analysis 13

Results **15**

Discussion **18**

Acknowledgements **22**

Citations **23**

Abstract

Physical trauma is the most frequent cause of death for people under the age of 45, accounting for approximately 30,000 deaths in Germany each year. Polytrauma (PT) in combination with hemorrhagic shock (HS) has been shown to severely impede PT recovery outcomes in clinical cohort studies and elevates biomarkers of cell injury, including membrane integrity proteins and proinflammatory signaling proteins. We hypothesized that systemic damage to the gut epithelium, in particular, would induce substantial changes to the composition of the gut microbiome and that the gut microbiome represents a potential non-invasive therapeutic target to improve recovery outcomes. A review of the literature demonstrates that little is known about the effects of PT, let alone PT and HS in tandem, on the microbiome aside from changes in alpha- and beta-diversity within the first 72 h of injury. We find that alpha-diversity in several metrics of microbial richness are inversely associated with inflammatory markers in the gastrointestinal tract, specifically C5a in the jejunum and colon (abundance-based coverage estimator, Pearson's $r = –0.332$, $p < 0.05$; Menhinick's richness index, Pearson's $r = –0.372$, $p < 0.05$). Additionally, alpha-diversity metrics of evenness are positively associated with C5a measured in mucosal swabs of the jejunum (Lladser's point estimate, Pearson's $r = 0.464$, $p < 0.01$; Heip's evenness, Pearson's $r = 0.355$, $p < 0.05$). These correlational analyses indicate that our preclinical model of polytrauma, despite inflicting no direct injuries to the gut, induces extensive inflammation in the small intestine and affects the microbiome by reducing bacterial abundance, targeting potentially beneficial bacteria necessary for recovery. We found no significant differences in community-wide analyses of beta diversity or taxonomic composition. This indicates that the gut microbiome immediately (within 3 h) responds to PT and HS in a highly standardized preclinical model and may be associated with key bacterial species that may facilitate increased morbidity and mortality.

Introduction

Physical trauma is the most frequent cause of death for people under the age of 45, accounting for approximately 30,000 deaths in Germany each year (Mutschler and Marzi, 1996). Hemorrhagic shock (HS) frequently accompanies severe injuries observed in polytrauma (PT); the additive effects of HS on PT remains associated with high morbidity and mortality rates despite modern treatments and damage control strategies (Wen et al., 2013). Clinical cohort studies have noted that PT, in which multiple body regions are severely damaged, frequently affects the lungs, brain, and endothelium tissue (Shultz et al., 2015; Wu et al., 2016; Yang et al., 2016; Denk et al., 2018). Although the mechanisms defining the severity of trauma-related complications have not been understood well until recently, studies suggest that exaggerated systemic inflammation is an important factor in the negative prognosis of trauma outcomes. The combination of thorax trauma with subsequent sepsis has, for instance, shown that overshooting immune responses substantially promote the development of acute lung injury (ALI) following trauma in mice (Perl et al., 2012). In line with these findings, human studies indicate that the development of multiple organ failure (MOF) and subsequent mortality is associated with exaggerated local or systemic inflammation at an early time point following trauma (Roumen et al., 1993; Meduri et al., 1995). Similarly, HS-mediated hyper-inflammation precedes a negative post-trauma course, as represented by sepsis and MOF (Angele et al., 2008).

Given these findings, factors promoting immune activation may also potentially affect an individuals' vulnerability to complications following physical traumatization. We recently established a mouse model of severe injury and blood loss (Denk et al., 2018). PT was induced

by a combination of closed traumatic head injury (TBI), blunt thorax trauma (TXT), soft tissue injury and femur fracture (Denk et al., 2018). The combination of PT with severe HS (blood pressure maintained at 30 mmHg for 60 min) increased histological lung injury, pulmonary edema, neutrophil influx, plasma clara cell protein 16 (CCL-16) and increased demand of catecholamine support to ensure mean arterial blood pressure (MAP) restoration (Denk et al., 2018). Moreover, HS contributed to the systemic release of interleukin-6 (IL-6; Denk et al., 2018) into the plasma and promoted intestinal damage and barrier dysfunction (reduced expression of tight junction protein zonula occludens protein-1 (ZO-1)) in PT+HS animals (Wrba et al., 2019).

Besides genetics (Heap and van Heel, 2009), aging (Ferrucci and Fabbri, 2018), and obesity (Rodriguez-Hernandez et al., 2013), one factor influencing overactive immune responses is the composition of the intestinal microbiome. For instance, alterations in the gut flora have often been related to abnormal production of cytokines (Paun et al., 2016). Human studies further indicate that inflammatory-related pathologies like inflammatory bowel disorder (IBD) often come along with changes in the composition of intestinal microbes (De Palma et al., 2014). In line with these findings, additional studies have shown that colonizing germ-free mice with the gut microbiota of IBD patients results in an increase in barrier dysfunction and innate immune activation in recipient animals (De Palma et al., 2017). Moreover, in the context of physical trauma, numerous studies demonstrate that different forms of injury affect the diversity of the gut microbiome. Human studies, for example, indicate that the grade of critical illness correlates with phylogenetic alterations of the intestinal microbiome (Shimizu et al., 2006). Bacterial dysbiosis triggered by trauma- or surgical injury-induced changes in the

gastrointestinal milieu is further associated with systemic inflammation (Patel et al., 2016) and intestinal dysfunction is also a common characteristic of physical traumatization of the brain (Bansal et al., 2009).

Given all these findings, it is substantially likely that microbial changes in the gut are also part of the pathophysiological consequences observed in our experimental model of PT and HS. Therefore, we investigated i) if there are measurable trauma-induced alterations in the intestinal microbiome of mice exposed to our polytrauma model, and ii) if these potential changes are in relation to inflammatory parameters. To achieve these aims, we analyzed the microbial diversity of caecal fecal samples taken from animals of our previously published studies (Denk et al., 2018; Wrba et al., 2019) employing 16 small subunit ribosomal RNA (16S rRNA) gene sequencing, and correlated the microbial diversity with the individual immunological parameters assessed in each animal.

Materials and Methods

Animals

C57BL/6J mice aged 8 to 9 weeks old (Jackson Laboratories, Bar Harbour, Maine, USA) with a mean body weight of 25 g (± 2.5 g) were randomly divided into the following groups with n = 8 animals/group: polytrauma (PT), hemorrhagic shock (HS), polytrauma + hemorrhagic shock (PT+HS), anaesthetized and catheterized-sham controls (Sham) and untreated control animals (Ctrl). Mice were anaesthetized with 2.5% sevoflurane (Sevorane Abbott, Wiesbaden, Germany)/97.5% oxygen, which was continued during the trauma-hemorrhagic procedure and during the whole observation period. For analgesia, 0.03 mg/kg buprenorphine was administered

by subcutaneous injection. The study protocol for the murine PT model with HS was approved by the University Animal Care Committee and the Federal Authorities for animal research, Tuebingen, Germany (No. 1194). Moreover, all experiments were performed in adherence to the National Institute of Health *Guide for the Care and Use of Laboratory Animals*.

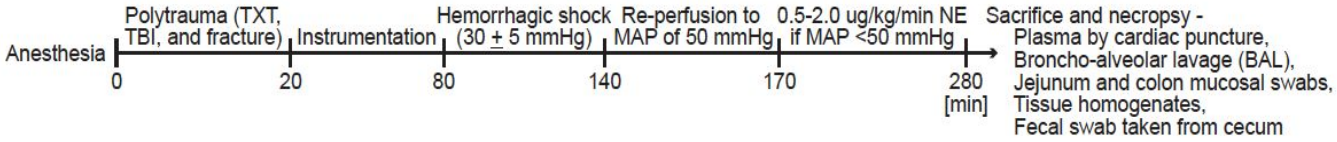

Figure 1. Scheme of the study design of the murine polytrauma (PT) model with hemorrhagic shock (HS): mice were randomly subjected to PT, HS, or PT + HS procedures. Abbreviations: HR, heart rate; MAP, mean arterial blood pressure.

Induction of PT and HS

Ten days following delivery, mice were randomly divided into five different experimental groups (n = 8 animals per experimental group): polytrauma (PT), hemorrhagic shock (HS), polytrauma + hemorrhagic shock (PT + HS), anaesthetized and catheterized-only controls (Sham), and non-treated control (Ctrl) animals. All mice were anaesthetized using 2.5% inhaled sevoflurane (Sevorane Abbott, Wiesbaden, Germany). Ctrl animals were euthanized by cardiac puncture directly after induction of anesthesia. For Sham, PT, HS, and PT+HS animals, anesthesia was continued throughout the whole experimental procedure. For analgesia, mice received subcutaneous buprenorphine (0.05 mg/ml s.c., Temgesic, RB Pharmaceutics, Slough, UK). The PT procedure was performed as previously described (Denk et al., 2018; Wrba et al., 2019; Fig. 1). Briefly, PT was induced by application of a blunt bilateral chest trauma (TXT), closed head injury (TBI) and a distal femur fracture accompanied by soft tissue injury.

Following PT induction, mice were incised at the shaved and cleaned left hind limb and a catheter (Föhr Medical Instruments, Seeheim/Ober-Beerbach, Germany) was inserted microsurgically into the femoral artery. This allowed the monitoring of the blood pressure by a blood pressure analyzer (Data Sciences International, DSI, St. Paul, Minnesota, USA) and a controlled blood loss to induce HS. Another incision was created along the ventral cervical skin into which a catheter was inserted into the jugular vein, which enabled us to resuscitate animals and control the infusion of catecholamines. The full HS procedure was also performed as previously described (Denk et al., 2018; Wrba et al., 2019): briefly, mice were bled for 5 to 10 min to reach a mean blood pressure of 30 mmHg (±5 mmHg) which was kept stable for 60 min. After hemorrhage, mice were resuscitated with a balanced electrolyte solution (Cat. no. H7 1340064, Jonosteril®, Servoprax, Wesel, Germany) via the jugular vein using 4-fold of the volume of the drawn blood over 30 min. After termination of this procedure, animals underwent a 2 h observation period. Thereby, animals were subjected to a preset protocol, adjusting anesthesia and norepinephrine support (0.01 – 0.12 µg/kg/min; Sanofi, Frankfurt am Main, Germany) in a standardized manner to maintain a mean arterial blood pressure (MAP) of 50 mmHg. The amount of transfused fluid, norepinephrine received, as well as blood hemoglobin (Hb) was documented for each animal.

Plasma, bronchoalveolar lavage (BAL), and fecal endpoints

Four hours after PT, EDTA blood was drawn by cardiac puncture. Plasma was obtained by centrifugation (5 min at 500 x *g* and 4 °C) and stored at –80 °C until total protein analysis, cytokines, and endothelial membrane proteins of interest could be measured via enzyme-linked immunosorbent assay (ELISA): IL-6, chemokine ligand 1 (KC), junctional adhesion molecule A

(JAM-A), high motility group box 1 (HMGB1), syndecan 1, S100 calcium-binding protein B (S100B), mucin-2, CC16, neutrophil gelatinase-associated lipocalin (NGAL), glial fibrillary acidic protein (GFAP), monocyte chemoattractant protein-1 (MCP-1), intestinal fatty acid binding protein (i-FABP), urea, liver fatty acid binding protein (L-FABP), claudin 5, complement component C3a (C3a). Following final blood draw, additional tissue samples were taken for further analysis during necropsy. In detail, bronchoalveolar lavage (BAL) was collected for the assessment of total protein, IL-6, KC, JAM-A, and HMGB1. Mucus from the jejunum and colon, as well as tissue homogenates without mucus, respectively, were used for the assessment of C3a, C5a, IL-6; jejunum and colon tissue claudin 5, occludin, KC, and JAM-A were also quantified. Finally, the caecum was opened aseptically for the removal of fecal samples for microbial analysis. Fecal samples were stored in sterile tubes at –80 °C until further analysis. Some readouts assessed in these animals (total protein, IL-6, and HMGB1 in BAL and plasma; CC16, GFAP, i-FABP and creatinine in plasma only) have been reported previously (Denk et al., 2018; Wrba et al., 2019).

Preparation of BAL fluids

For the collection of lung fluids via BAL, the trachea was dissected and cannulated, the left lung was clamped, and the right lung was flushed 3 times with 0.5 ml PBS containing a 1:1000 broad spectrum protease inhibitor (Cat. no. P8340, Sigma-Aldrich, St. Louis, Missouri, USA). The BAL fluids were then centrifuged (10 min, at 450 x *g* and 4 °C) and the supernatant was stored at –80 °C until analysis.

Jejunum and colon mucus extraction and homogenization of jejunum and colon tissue

For mucus collection, approximately 10 cm of the jejunum and the entire colon were extracted, flushed with 10 ml ice-cold phosphate-buffered saline (PBS) each, and dissected longitudinally. Mucus was collected into a siliconized 1.5 ml microcentrifuge tube (Cat. no. 416556, Bio Plas, San Rafael, CA, USA) using a glass cover slip. After centrifugation (10 min, at 6000 x *g* and 4 °C), the supernatant was discarded and mucus was stored at –80 °C. The remaining jejunum and colon tissues were homogenized and sonified in PBS containing a 1:1000 broad spectrum protease inhibitor as described previously in the BAL preparation. After centrifugation (15 min, at 16,000 x *g* and 4 °C), the supernatant was collected and stored at –80 °C until further analysis.

Protein assay

Measurement of plasma and BAL total protein was performed as described before (Denk et al., 2018). Briefly, the total protein concentration in the plasma and BAL samples was quantified using a bicinchoninic acid Protein Assay Kit (Cat. no. 23227, Pierce Inc., Rockford, Illinois, USA) according to the manufacturer's instructions.

Enzyme-linked immunosorbent assay (ELISA)

ELISAs and sequential ELISA measurements were performed as described before (Denk et al., 2018; Wrba et al., 2019; Remick and Love, 2006). Briefly, the following ELISA kits were used according to the manufacturer's recommendations: BD OptEIA Mouse IL-6 ELISA Set (BD Pharmingen, San Diego, CA, USA), high mobility group box 1 protein (HMGB1) ELISA

Kit (IBL International, Hamburg, Germany), Mouse CC16 ELISA kit, Mouse S100B ELISA kit, Mouse NGAL ELISA kit, and Mouse L-FABP ELISA kit (all Lifespan Biosciences Inc, Seattle, WA, USA). The measured parameter concentration of the jejunum and colon mucus, as well as the jejunum and colon tissue homogenate, were calculated relative to the total protein concentration in the corresponding sample.

Quantification of plasma creatine

For the measurement of plasma creatinine, 50 µl of internal standard solution consisting of 5 µg/mL of $^{2}H_{3}$-creatinine (Cat. no. D-3689, CDN isotopes, Pointe-Claire, Quebec, Canada) were added to 10 µl of each mouse plasma sample. After mixing, samples were equilibrated for 10 min at room temperature, deproteinized by addition of 500 mL acetonitrile and centrifuged for up to 5 min at 13,000 x *g*. Twenty-five µl of the supernatant were directly used for urea quantification. The residual sample was evaporated to dryness, reconstituted in 500 mL 0.01% formic acid, and extracted over an anion exchange column (Phenomenex®, Aschaffenburg, Germany). After washing with HPLC-grade water and methanol, creatinine was recovered using a 9:1 methanol:formic acid solution. The trimethylsilyl-derivative of creatinine was prepared by adding 100 mL of 2:1 acetonitrile:*N,O*-Bis(trimethylsilyl)trifluoroacetamide (BSTFA) to the dry sample and heating to 80 °C for 60 min. Analyses were carried out on an Agilent 5890/5970 gas chromatography/ mass spectrometry system, housing an Optima-5MS® capillary column (Macherey-Nagel, Düren, Germany). Creatinine analysis was carried out by monitoring ions *m*/*z* 329 and 332 for analytes and internal standard. For quantification, six-point calibration curves were used (Smith-Palmerm, 2002).

Bacterial DNA extraction and generation of 16S rRNA gene V4 amplicons

Bacterial genomic DNA extraction, hypervariable region 4 (V4) amplicon generation from the 16S rRNA gene and amplicon preparation for sequences were performed according to protocols benchmarked for the Earth Microbiome Project (EMP) and can be found on the EMP website (http://www.earthmicrobiome.org/emp-standard-protocols/). Briefly, bacterial genomic DNA was extracted from samples using the DNeasy® PowerSoil® 96-well DNA isolation kit (Cat. no. 12955-4, Qiagen Laboratories, Hilden, Germany) according to manufacturer's instructions. Marker genes in isolated DNA were PCR-amplified in triplicate from each sample, targeting V4 of the 16S rRNA gene, modified with a unique 12-bp sequence identifier for each sample and the Illumina adapter, as previously described by Caporaso et al. (2012).

The PCR mixtures contained 13 µl Mo Bio PCR water, 10 µl 5'-HotMasterMix, 0.5 µl each of the barcoded forward and reverse primers (515-bp forward: 5'-GTGCCAGCMGCCGCGGTAA-3'; 806-bp reverse: 5'-GGACTACHVGGGTWTCTAAT-3'; 10 µM final concentration, Integrated DNA Technologies, San Diego, CA, USA), and 1.0 µl genomic DNA. Reaction mixtures were held at 94 °C for 3 min, followed by 35 cycles of amplification (94 °C for 45 s, 50 °C for 1 min, and 72 °C for 1.5 min), followed by a final extension at 72 °C for 10 min. After amplification, the DNA concentration was quantified using PicoGreen™ double-stranded DNA (dsDNA) reagent in 10 mM Tris buffer (pH 8.0) (Cat. no. P11496, Thermo Fisher Scientific). A composite sample for sequencing (16S rRNA gene library) was created by combining equimolar ratios of

amplicons from the individual samples, followed by ethanol precipitation to remove any remaining contaminants and PCR artifacts.

16S rRNA gene sequence data analysis

Pooled amplicons were sequenced at the BioFrontiers Next Generation Sequencing Core Facility at the University of Colorado Boulder using the Illumina MiSeq® platform. The 16S rRNA gene library concentration was measured using the HiSens Qubit dsDNA HS assay kit (Cat. No. Q32854, ThermoFisher Scientific, Waltham, MA, USA). A total of 6 pM of the 16S rRNA gene library combined with 0.9 pM (15%) PhiX sequencing library control v3 (Cat. no. FC-110,3001, Illumina Inc., San Diego, CA, USA) was sequenced with 150-bp paired-end reads on an Illumina MiSeq® sequencing system using a MiSeq reagent kit v2 (300 cycles; Cat. no. MS-102-2002, Illumina Inc.). FASTQ files for reads 1 (forward), 2 (reverse), and the index (barcode) read were generated using the BCL-to-FASTQ file converter bcl2fastq (ver. 2.17.1.14, Illumina, Inc.).

Sequencing data were prepared and analyzed using the Quantitative Insights Into Microbial Ecology microbiome analysis pipeline (QIIME2 ver. 2020.2, http://qiime2.org; (Bolyen et al., 2019). Mapping files and raw sequencing information are publicly available on the microbiome study management platform Qiita (http://qiita.ucsd.edu/study/description/15093; (Gonzalez et al., 2018). Briefly, raw sequencing results were quality-filtered and demultiplexed using the DADA2 microbiome pipeline (available at https://github.com/benjjneb/dada2), which describes microbial communities using unique sequence variants present in the data, known as amplicon sequence variants (ASVs) (Callahan et al., 2016). In brief, sequence reads were first

filtered using DADA2's recommended parameters (i.e., an expected error threshold of 2 combined with the trimming of 10 nucleotides from the start and end of each read). Filtered reads were then de-replicated and de-noised using DADA2 default parameters. De-replication combines identical reads into unique sequences and constructs consensus quality profiles for each combined lot of sequences; the consensus quality profiles then inform the de-noising algorithm which infers error rates from samples and removes identified sequencing errors from the samples. After building the ASV table and removing chimeras, taxonomy was assigned using the Ribosomal Database Project (RDP) classifier (v2.2) (Wang et al., 2007) natively implemented in DADA2 and trained against the Greengenes reference database (13.8) (Werner et al., 2011; McDonald et al., 2012). A phylogenetic tree was built using FastTree (v2.1.3) (Price et al., 2010) from a multiple sequence alignment made with the PyNAST alignment tool (Caporaso et al., 2010a), against the Greengenes Core reference alignment (DeSantis et al., 2006). Quality filtering resulted in an output feature table of 195,873 high quality reads in all 36 samples at 1,156 sequences per sample following rarefaction.

Microbiome data analysis

Microbial community structure was characterized using measures of alpha-diversity (within-sample) and beta-diversity (between-samples). Metrics of alpha-diversity included, but were not limited to, the number of distinct features to represent species richness, Shannon's diversity index to quantify species abundance and evenness (Shannon et al., 1949), and Faith's Phylogenetic Diversity, which measures the total length of branches in a reference phylogenetic tree for all species in a given sample (Faith, 1992). Pearson's correlation tests using an

alpha-threshold of 0.05 on the rarefied feature table were ran and included below only if the test was significant both before and after an extreme outlier in the dataset was removed.

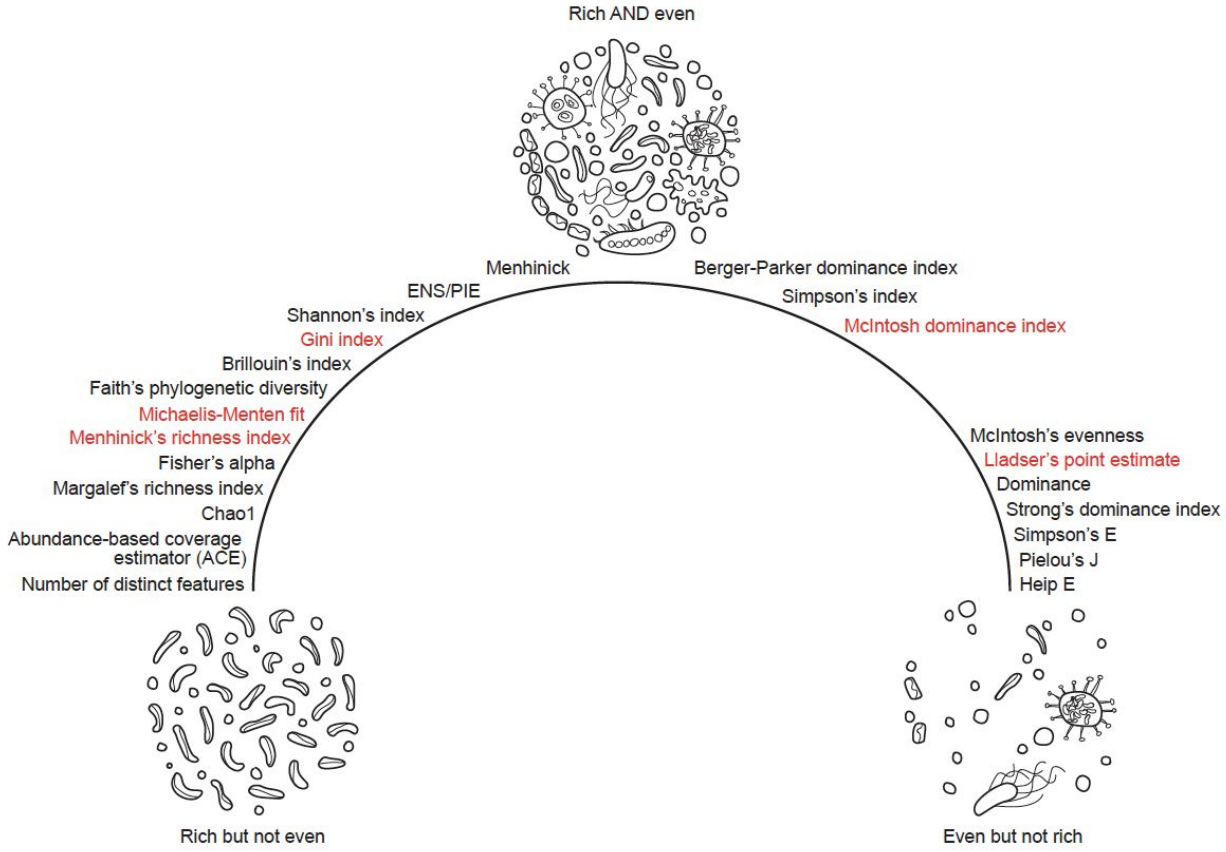

Figure 2. Alpha-diversity metrics in the Quantitative Insights Into Microbial Ecology (QIIME2) analysis pipeline ranked by feature loadings on a richness - evenness scale as in Hagerty et al. (2020). Metrics in red text were not included in the rank-order analysis performed by Hagerty et al. (2020) but are inserted here based on descriptions of each method as provided by their original publications and were used in this study.

Beta-diversity was calculated using unweighted UniFrac distances (Lozupone and Knight, 2005; Lozupone et al., 2007; Lozupone et al., 2011) depicting community-wide differences in microbial composition amongst cecal samples. Output distance matrices were ordinated using principal coordinate analyses (PCoA) and visualized using EMPeror (Vázquez-Baeza et al., 2013). Statistical significance of beta-diversity distances between groups was assessed using permutational analyses of variance (PERMANOVA) with 999 permutations.

We investigated differences in ASV abundance between categorical data grouped as low vs. high or low vs. medium vs. medium-high vs. high using the analysis of composition of microbiomes (ANCOM) framework (Mandal et al., 2015). ANCOM accounts for the compositional nature of the taxa relative abundances and is based on the analysis of difference in pairwise log-ratios of microbial OTU abundances/relative abundances, between comparison groups of interest. For each taxon, we computed a statistic indicating the number of significantly different pairwise log-ratios while controlling for false discoveries. We applied ANCOM with a Benjamini-Hochberg correction at an alpha-threshold of 0.05.

Results

Alpha-diversity analysis

We find that alpha-diversity in several metrics of microbial richness are inversely associated with inflammatory markers in the gastrointestinal tract, specifically C5a in the jejunum (abundance-based coverage estimator, Pearson's $r = –0.332$, $p < 0.05$; Chao1, Pearson's $r = –0.332$, $p < 0.05$) and in the colon (Menhinick's richness index, Pearson's $r = –0.372$, $p < 0.05$). Interestingly, analysis of evenness metrics show that increased jejunum C5a concentrations are inversely associated with microbial alpha-diversity (Strong's dominance index, Pearson's $r = –0.406$, $p < 0.05$). As a proof-of-concept, analysis of the Berger-Parker dominance index, considered to be an alpha-diversity metric representing a balance of both richness and evenness (Hagerty et al., 2020), demonstrated that jejunum C5a concentrations were positively associated with this metric (Pearson's $r = 0.336$, $p < 0.05$). Additionally, alpha-diversity metrics of evenness were positively associated with C5a measured in mucosal

swabs of the jejunum (Lladser's point estimate, Pearson's $r = 0.464$, $p < 0.01$; Heip's evenness, Pearson's $r = 0.355$, $p < 0.05$).

Analysis of biomarkers of cellular damage, such as plasma KC and CC-16 (normally found only in the lungs), reveal that increasing concentrations of these DAMPs are positively associated with Menhinick's richness index (Pearson's $r = 0.346$ and 0.333 respectively, $p < 0.05$ in both instances). Plasma levels of syndecan, which indicates cell membrane degradation and necrosis (Torres, 2016), demonstrates that evenness as measured by Lladser's point estimate also increases (Pearson's $r = 0.354$, $p < 0.05$). Other indicators of localized inflammation, such as HMGB1 in the BAL, are also positively associated with both microbial richness (Menhinick's richness index, Pearson's $r = 0.419$, $p < 0.05$) and evenness (Lladser's point estimate, Pearson's $r = 0.368$, $p < 0.05$). Colon JAM-A, the junctional adhesion molecule, was also positively correlated with metrics of evenness such as Strong's diversity index (Pearson's $r = 0.341$, $p < 0.05$).

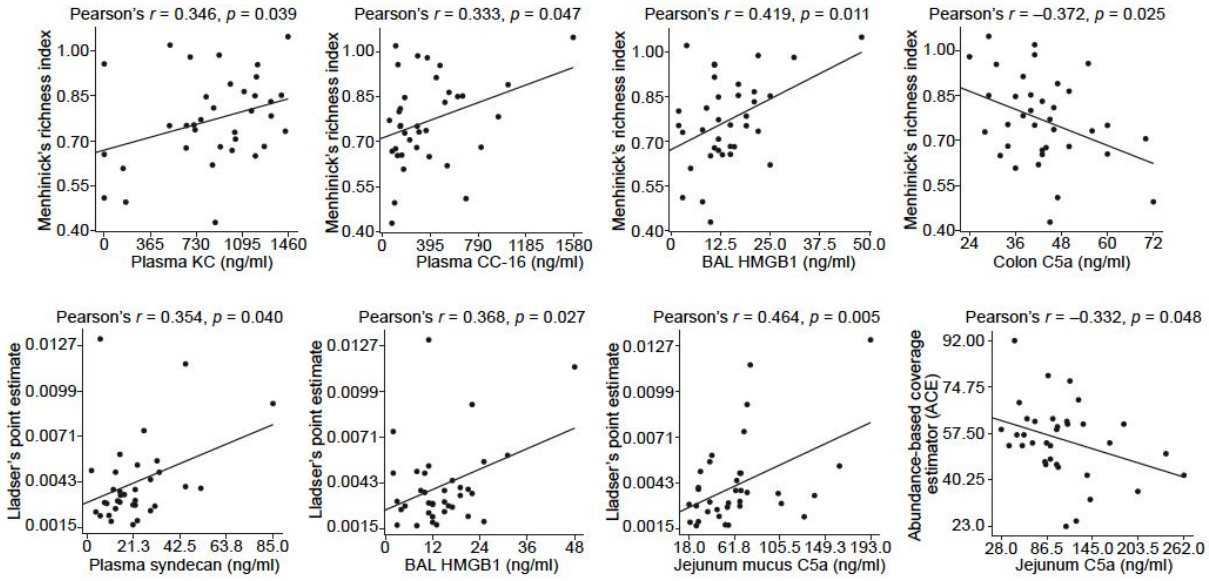

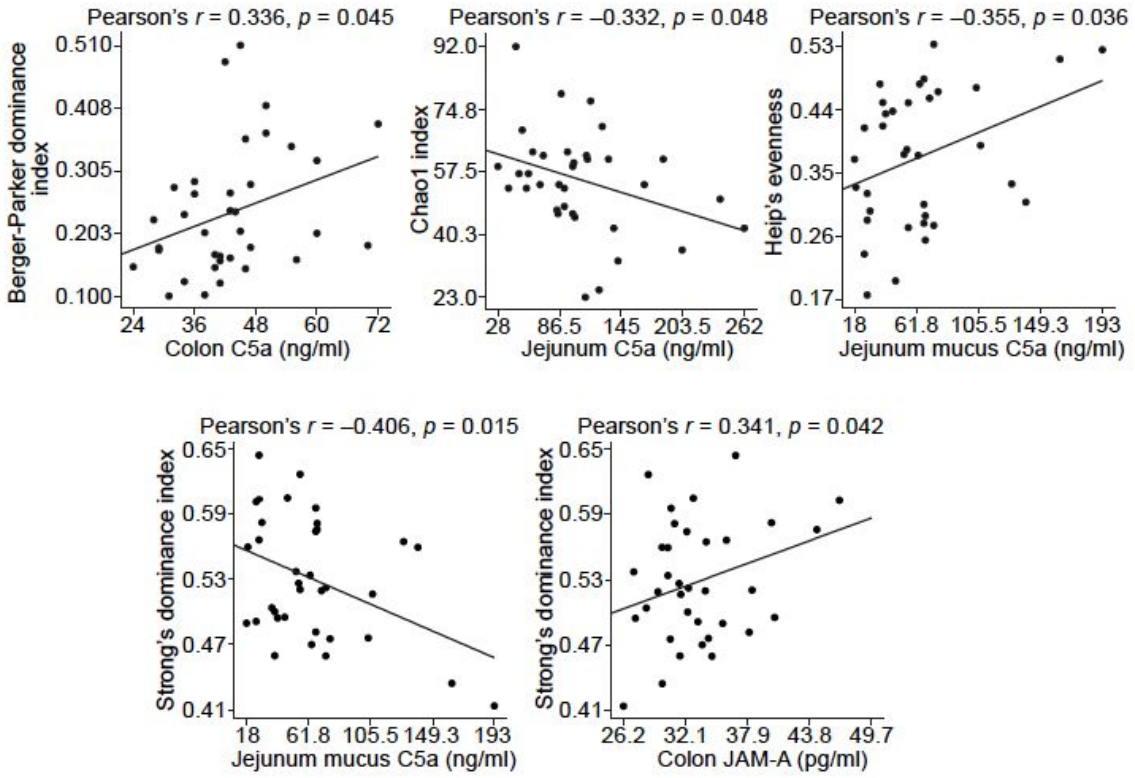

Figure 3. Pearson's correlation analyses of microbial alpha-diversity and several inflammatory proteins and membrane damage-associated molecular patterns (DAMPs) known to be increased in the preclinical polytrauma (PT) model established by Denk et al. (2018). Abbreviations: BAL, bronchoalveolar lavage; C5a, complement component 5a; CC-16, clara cell protein 16; DAMP, damage-associated molecular pattern; HMGB1, high mobility group box 1 protein; JAM-A, junctional adhesion molecule A; KC, chemokine ligand 1; PT, polytrauma.

Beta-diversity and taxa-driving differences

Following the results from our alpha-diversity analyses in Pielou's evenness, Faith's phylogenetic diversity, number of distinct features, and Shannon's diversity index, we ran permutational analyses of variance (PERMANOVAs) on the unweighted and weighted UniFrac distance matrices. Analysis of BAL IL-6, colon IL-6, jejunum C5a, plasma IL-6 and claudin 5, and experimental manipulation (collapsed trauma vs. no-trauma categories, and uncollapsed groups as described above) demonstrated that there were no significant differences in microbial communities from samples stratified as above. ANCOM of differentially abundant ASVs that

discriminate between low and high BAL IL-6, colon IL-6, jejunum C5a, plasma IL-6 and claudin 5, and experimental manipulation (collapsed trauma vs. no-trauma categories, and uncollapsed groups as described above) demonstrated that no taxa were significantly different. However, we did note during the analysis of colon IL-6 had some taxa that were differentially abundant prior to Benjamini-Hochberg correction, with W effect sizes of greater than 1.

Discussion

Our study provided new insights about the role of the proximal gut microbiome in healthy and mice with polytrauma. We identified that the microbiome's alpha-diversity in metrics of both richness and evenness was correlated to several membrane integrity proteins that are DAMPs, or biomarkers of systemic damage to the epithelium. We also identified a key biomarker of inflammation, namely C5a, in the gastrointestinal tract that was a significant correlate of evenness and richness, despite no direct physical trauma inflicted upon the jejunum or colon in this preclinical model. The relationship between correlates of richness and evenness with these inflammatory and membrane-integrity signals demonstrate that changes in the microbiome cannot be adequately encapsulated through a single alpha-diversity metric. We've found that alpha-diversity analyses require a composite of several tests to adequately describe the flux in gut communities that are induced by trauma. Additionally, these changes have no relationship to beta-diversity, as evidenced by the lack of significant differences determined by permutational ANOVAs between microbial communities of the stratified samples. These findings indicate that the inflammatory phenotype induced by PT, and exacerbated in the PT+HS model established by Denk et al. (2018), are associated with changes in the gut microbiome and

can be traced back to changes in the relative abundances of bacteria belonging to several clusters of previously uncharacterized species.

These results, in line with previous findings from our lab (Denk et al., 2018; Wrba et al., 2019), extensively characterize the gut microbiome's response to increasing systemic damage to the epithelium induced by PT+HS. The microbiome (not just the bacterial assemblage located in the gastrointestinal tract, but also in the skin) has been shown in several preclinical models of autoimmune disease and clinical cohort studies to respond to DAMPs released by injured cells. Previous literature has characterized the extent to which the intestinal epithelial barrier's luminal and mucosal components are laced with innate immune cells and neuroendocrine signaling cells (Paolella et al., 2014). Of particular interest to us are goblet cells in the proximal gut, which regulate the release of phagocytic cells such as macrophages and dendritic cells into the gut mucosa, and are likely to directly interface with the microbiome (Saltzman et al., 2018). Damage-associated molecular patterns, such as KC and CC-16, released into systemic circulation would activate phagocytic cells in the entire body to sense and launch immune responses to PT. Additionally, the gut microbiome has been shown to maintain tight junctions in the epithelium by regulating the expression of ZO-1 proteins and were damaged by PT (Cani et al., 2009; Halbgebauer et al., 2018). It is entirely possible that the gut microbiome's response to DAMPs, therefore, enhances the immune response to PT to the detriment of the host.

Our composite analysis of changes in several alpha-diversity metrics in response to jejunum C5a has shown that the microbiome is responsive to direct inflammatory signals, in addition to indirect responses to DAMPs as discussed previously (Fig. 3). The complement fragment C5a has a critical role in intestinal tissue inflammation and damage when subjected to

HS in the absence of other trauma. In fact, studies demonstrate C5a-deficiency protects mice against HS by reducing injury severity scores 8 times less than in wildtype control mice (Fleming et al., 2008). The authors predicted that therapeutics targeting C5a would be useful in treating HS-associated injury; here, we show that the microbiome is immediately responsive to C5a concentrations in the intestinal tissue and mucosae, and serves as a promising therapeutic target in the same vein. Our data indicate that as C5a increases in the jejunum tissue and follows a concentration gradient in the progression of trauma into the mucosa, microbial alpha-diversity increases, suggesting that certain bacteria selectively proliferate in response to this innate immunogenic signal. These bacteria may be potential drivers of the microbiome's response to trauma.

We find that community-wide shifts in microbial composition, as described by beta-diversity analysis of the unweighted and weighted UniFrac distances (Lozupone et al., 2011), do not occur within 2 h of PT+HS. A recent clinical cohort study of patients admitted to the intensive care unit with and without polytrauma found no detectable differences in gut microbial community diversity upon admittance (0 h after trauma), but that differences quickly developed within 72 h (Howard et al., 2017). Our data support these findings in the preclinical setting, with the added caveat that minor changes in bacterial abundance do not always translate into immediate global changes in microbiome community composition. Similarly, ANCOM analyses of the rarefied feature table indicate that there were no significant standalone taxa that induced global changes to the cecal microbiome. Given these results, we hypothesize that the acute model of PT+HS induces changes in specific bacterial abundances but that a longitudinal study extending several hours past the induction of PT+HS is required to identify and evaluate

which species are the first responders to intestinal damage, thereby driving and sustaining changes in microbial composition throughout the course of recovery.

Several studies have demonstrated that critical illness correlates with significant alterations in microbial populations in models of severe injury leading to sepsis (McDonald et al., 2016; Earley et al., 2015; Krezalek et al., 2016). We've shown in this study that preclinical models of PT+HS are associated with the systemic expression of DAMPs and localized expression of C5a in the intestinal tissue and mucosa, revealing a role that has been previously uncharacterized of the microbiome in the pathophysiological course of trauma and shock. Our analysis of the gut microbiome has led to a better understanding of how we can create non-invasive therapeutic approaches that directly combat and intervene in pathological clinical trajectories.

Acknowledgements

This work was supported by a grant from the Biological Sciences Initiative (BSI) at CU Boulder to Sandra A. Appiah. I'd like to thank Dr. Markus Huber-Lang, Dr. Stefan O. Reber, Dr. Dominik Langgartner, Dr. Rebecca Halbegebauer, and the rest of the Polytrauma team for giving me the opportunity to support this project. I'd like to thank my mentor, Dr. Christopher A. Lowry, and Dr. Brian DeDecker, Dr. Heidi Day, and Dr. Nancy Guild for sitting on my committee. I'd also like to thank Christine Foxx for her mentorship and guidance during this process.

References

Angele, M.K., Schneider, C.P., and Chaudry, I.H. (2008). Bench-to-bedside review: latest results in hemorrhagic shock. *Critical Care, 12*(4)**,** 218. doi: 10.1186/cc6919.

Bansal, V., Costantini, T., Kroll, L., Peterson, C., Loomis, W., Eliceiri, B., et al. (2009). Traumatic brain injury and intestinal dysfunction: uncovering the neuro-enteric axis. *Journal of Neurotrauma, 26*(8)**,** 1353-1359. doi: 10.1089/neu.2008-0858

Bolyen, E., Rideout, J.R., Dillon, M.R., Bokulich, N.A., Abnet, C.C., Al-Ghalith, G.A., et al. (2019). Reproducible, interactive, scalable and extensible microbiome data science using QIIME 2. *Nature Biotechnology*, *37*(8), 852-857. doi: 10.1038/s41587-019-0209-9

Callahan, B.J., McMurdie, P.J., and Holmes, S.P. (2017). Exact sequence variants should replace operational taxonomic units in marker-gene data analysis. *The International Society of Microbial Ecology Journal, 11*(12), 2639-2643. doi: 10.1038/ismej.2017.119

Cani, P.D., Possemiers, S., Van de Wiele, T., Guiot, Y., Everard, A., Rottier, O., et al. (2009). Changes in gut microbiota control inflammation in obese mice through a mechanism involving GLP-2-driven improvement of gut permeability. *Gut*, *58*(8), 1091-1103. doi: 10.1136/gut.2009.179325

Caporaso, J.G., Bittinger, K., Bushman, F.D., DeSantis, T.Z., Andersen, G.L., and Knight, R. (2010a). PyNAST: a flexible tool for aligning sequences to a template alignment. *Bioinformatics, 26*(2)**,** 266-267. doi: 10.1093/bioinformatics/btp636.

Caporaso, J.G., Paszkiewicz, K., Field, D., Knight, R., and Gilbert, J.A. (2012). The western english channel contains a persistent microbial seed bank. *The International Society of Microbial Ecology Journal, 6*(6)**,** 1089-1093. doi: 10.1038/ismej.2011.162.

De Palma, G., Collins, S.M., Bercik, P., and Verdu, E.F. (2014). The microbiota-gut-brain axis in gastrointestinal disorders: stressed bugs, stressed brain or both? *Journal of Physiology, 592*(14)**,** 2989-2997. doi: 10.1113/jphysiol.2014.273995.

De Palma, G., Lynch, M.D., Lu, J., Dang, V.T., Deng, Y., Jury, J., et al. (2017). Transplantation of fecal microbiota from patients with irritable bowel syndrome alters gut function and behavior in recipient mice. *Science Translational Medicine, 9*(379), eaaf6397. doi: 10.1126/scitranslmed.aaf6397.

Denk, S., Weckbach, S., Eisele, P., Braun, C.K., Wiegner, R., Ohmann, J.J., et al. (2018). Role of hemorrhagic shock in experimental polytrauma. *Shock, 49*(2)**,** 154-163. doi: 10.1097/SHK.0000000000000925.

DeSantis, T.Z., Hugenholtz, P., Larsen, N., Rojas, M., Brodie, E.L., Keller, K., et al. (2006). Greengenes, a chimera-checked 16S rRNA gene database and workbench compatible with ARB. *Applied and Environmental Microbiology, 72*(7)**,** 5069-5072. doi: 10.1128/AEM.03006-05.

Earley, Z.M., Akhtar, S., Green, S.J., Naqib, A., Khan, O., Cannon, A. R., et al. (2015). Burn injury alters the intestinal microbiome and increases gut permeability and bacterial translocation. *PloS One*, *10*(7). doi: 10.1371/journal.pone.0129996

Edgar, R.C. (2010). Search and clustering orders of magnitude faster than BLAST. *Bioinformatics, 26*(19)**,** 2460-2461. doi: 10.1093/bioinformatics/btq461.

Faith, D.P. (1992). Conservation evaluation and phylogenetic diversity. *Biological Conservation*, *61*(1), 1-10. doi: 10.1016/0006-3207(92)91201-3

Ferrucci, L., and Fabbri, E. (2018). Inflammageing: chronic inflammation in ageing, cardiovascular disease, and frailty. *Nature Reviews Cardiology, 15*(9)**,** 505-522. doi: 10.1038/s41569-018-0064-2.

Fleming, S.D., Phillips, L.M., Lambris, J.D. & Tsokos, G.C. (2008) Complement component C5a mediates hemorrhage-induced intestinal damage. *Journal of Surgical Research*, *150*, 196-203. doi: 10.1016/j.jss.2008.02.010.

Gonzalez, A., Navas-Molina, J. A., Kosciolek, T., McDonald, D., Vázquez-Baeza, Y., Ackermann, G., et al. (2018). Qiita: rapid, web-enabled microbiome meta-analysis. *Nature Methods*, *15*(10), 796-798. doi: 10.1038/s41592-018-0141-9.

Hagerty, S.L., Hutchison, K.E., Lowry, C.A., Bryan, A.D. (2020). An empirically derived method for measuring human gut microbiome alpha diversity: demonstrated utility in predicting health-related outcomes among a human clinical sample. *PloS One*, *15*(3), e0229204.

Halbgebauer, R., Braun, C.K., Denk, S., Mayer, B., Cinelli, P., Radermacher, P., et al. (2018). Hemorrhagic shock drives glycocalyx, barrier and organ dysfunction early after polytrauma. *Journal of Critical Care, 44***,** 229-237. doi: 10.1016/j.jcrc.2017.11.025.

Heap, G.A., and van Heel, D.A. (2009). The genetics of chronic inflammatory diseases. *Human Molecular Genetics, 18*(R1)**,** R101-106. doi: 10.1093/hmg/ddp001.

Howard, B.M., Kornblith, L.Z., Christie, S.A., Conroy, A.S., Nelson, M.F., Campion, E.M., et al. (2017). Characterizing the gut microbiome in trauma: significant changes in microbial

diversity occur early after severe injury. *Trauma Surgery & Acute Care Open*, *2*(1), e000108. doi: 10.1136/tsaco-2017-000108

Krezalek, M. A., DeFazio, J., Zaborina, O., Zaborin, A., and Alverdy, J. C. (2016). The shift of an intestinal "microbiome" to a "pathobiome" governs the course and outcome of sepsis following surgical injury. *Shock, 45*(5), 475-482. doi: 10.1097/SHK.0000000000000534

Lozupone, C., and Knight, R. (2005). UniFrac: a new phylogenetic method for comparing microbial communities. *Applied and Environmental Microbiology*, *71*(12), 8228-8235.

Lozupone, C. A., Hamady, M., Kelley, S. T., and Knight, R. (2007). Quantitative and qualitative β diversity measures lead to different insights into factors that structure microbial communities. *Applied and Environmental Microbiology, 73*(5), 1576-1585. doi: 10.1128/AEM.01996-06

Lozupone, C., Lladser, M. E., Knights, D., Stombaugh, J., and Knight, R. (2011). UniFrac: an effective distance metric for microbial community comparison. *The International Society of Microbial Ecology Journal, 5*(2), 169-172. doi: 10.1038/ismej.2010.133

McDonald, D., Price, M.N., Goodrich, J., Nawrocki, E.P., DeSantis, T.Z., Probst, A., et al. (2012). An improved Greengenes taxonomy with explicit ranks for ecological and evolutionary analyses of bacteria and archaea. *The International Society of Microbial Ecology Journal, 6*(3)**,** 610-618. doi: 10.1038/ismej.2011.139.

McDonald, D., Ackermann, G., Khailova, L., Baird, C., Heyland, D., Kozar, R., ... & Knight, R. (2016). Extreme dysbiosis of the microbiome in critical illness. *mSphere*, *1*(4), e00199-16. doi: 10.1128/mSphere.00199-16

Meduri, G.U., Headley, S., Kohler, G., Stentz, F., Tolley, E., Umberger, R., et al. (1995). Persistent elevation of inflammatory cytokines predicts a poor outcome in ARDS. Plasma IL-1 beta and IL-6 levels are consistent and efficient predictors of outcome over time. *Chest, 107*(4)**,** 1062-1073. doi: 10.1378/chest.107.4.1062.

Mutschler, W., and Marzi, I. (1996). [Management of polytrauma]. *Zentralblatt fur Chirurgie, 121*(11)**,** 895.

Patel, J.J., Rosenthal, M.D., Miller, K.R., and Martindale, R.G. (2016). The gut in trauma. *Current Opinion in Critical Care, 22*(4)**,** 339-346. doi: 10.1097/MCC.0000000000000331.

Paun, A., Yau, C., and Danska, J.S. (2016). Immune recognition and response to the intestinal microbiome in type 1 diabetes. *Journal of Autoimmunity, 71***,** 10-18. doi: 10.1016/j.jaut.2016.02.004.

Perl, M., Hohmann, C., Denk, S., Kellermann, P., Lu, D., Braumuller, S., et al. (2012). Role of activated neutrophils in chest trauma-induced septic acute lung injury. *Shock, 38*(1)**,** 98-106. doi: 10.1097/SHK.0b013e318254be6a.

Paolella, G., Mandato, C., Pierri, L., Poeta, M., Di Stasi, M., and Vajro, P. (2014). Gut-liver axis and probiotics: their role in non-alcoholic fatty liver disease. *World Journal of Gastroenterology, 20*(42), 15518. doi: 10.3748/wjg.v20.i42.15518

Price, M.N., Dehal, P.S., and Arkin, A.P. (2010). FastTree 2--approximately maximum-likelihood trees for large alignments. *PLoS One, 5*(3)**,** e9490. doi: 10.1371/journal.pone.0009490.

Remick, K.J. and Love, J.J. (2006). Statistical modeling of storm‐level Kp occurrences. *Geophysical Research Letters*, *33*(16). doi: 10.1029/2006GL026687

Rodriguez-Hernandez, H., Simental-Mendia, L.E., Rodriguez-Ramirez, G., and Reyes-Romero, M.A. (2013). Obesity and inflammation: epidemiology, risk factors, and markers of inflammation. *International Journal of Endocrinology, 2013,* 678159. doi: 10.1155/2013/678159.

Roumen, R.M., Hendriks, T., van der Ven-Jongekrijg, J., Nieuwenhuijzen, G.A., Sauerwein, R.W., van der Meer, J.W., et al. (1993). Cytokine patterns in patients after major vascular surgery, hemorrhagic shock, and severe blunt trauma. Relation with subsequent adult respiratory distress syndrome and multiple organ failure. *Annals of Surgery, 218*(6)**,** 769-776. doi: 10.1097/00000658-199312000-00011.

Saltzman, E. T., Palacios, T., Thomsen, M., and Vitetta, L. (2018). Intestinal microbiome shifts, dysbiosis, inflammation, and non-alcoholic fatty liver disease. *Frontiers in Microbiology*, *9*, 61. doi: 10.3389/fmicb.2018.00061.

Shannon, C.E. (1949). Communication in the presence of noise. *Proceedings of the IRE*, *37*(1), 10-21.

Shimizu, K., Ogura, H., Goto, M., Asahara, T., Nomoto, K., Morotomi, M., et al. (2006). Altered gut flora and environment in patients with severe SIRS. *Journal of Trauma, 60*(1)**,** 126-133. doi: 10.1097/01.ta.0000197374.99755.fe.

Shultz, S.R., Sun, M., Wright, D.K., Brady, R.D., Liu, S., Beynon, S., et al. (2015). Tibial fracture exacerbates traumatic brain injury outcomes and neuroinflammation in a novel

mouse model of multitrauma. *Journal of Cerebral Blood Flow and Metabolism, 35*(8)**,** 1339-1347. doi: 10.1038/jcbfm.2015.56.

Vázquez-Baeza, Y., Pirrung, M., Gonzalez, A., and Knight, R. (2013). EMPeror: a tool for visualizing high-throughput microbial community data. *Gigascience*, *2*(1), 16. doi: 10.1186/2047-217X-2-16.

Wang, Q., Garrity, G.M., Tiedje, J.M., and Cole, J.R. (2007). Naive Bayesian classifier for rapid assignment of rRNA sequences into the new bacterial taxonomy. *Applied and Environmental Microbiology*, *73*(16), 5261-5267. doi: 10.1128/AEM.00062-07

Wen, Y., Yang, H., and Wei, W. (2013). The outcomes of 1120 severe multiple trauma patients with hemorrhagic shock in an emergency department: a retrospective study. *BMC Emergency Medicine, 13*(1), S6. doi: 10.1186/1471-227X-13-S1-S6

Werner, J.J., Koren, O., Hugenholtz, P., DeSantis, T.Z., Walters, W.A., Caporaso, J.G., et al. (2012). Impact of training sets on classification of high-throughput bacterial 16s rRNA gene surveys. *The International Society of Microbial Ecology Journal, 6*(1), 94-103. doi: 10.1038/ismej.2011.82

Wrba, L., Ohmann, J.J., Eisele, P., Chakraborty, S., Braumuller, S., Braun, C.K., et al. (2019). Remote intestinal injury early after experimental polytrauma and hemorrhagic shock. *Shock, 52*(4)**,** e45-e51. doi: 10.1097/SHK.0000000000001271.

Wu, X., Darlington, D.N., and Cap, A.P. (2016). Procoagulant and fibrinolytic activity after polytrauma in rats. *American Journal of Physiology: Regulatory, Integrative, and Comparative Physiology, 310*(4)**,** R323-329. doi: 10.1152/ajpregu.00401.2015.

Yang, L., Guo, Y., Wen, D., Yang, L., Chen, Y., Zhang, G., et al. (2016). Bone fracture enhances trauma brain injury. *Scandinavian Journal of Immunology, 83*(1)**,** 26-32. doi: 10.1111/sji.12393.